Seabirds reveal mercury distribution across the North Atlantic

Céline Albert, Børge Moe, Hallvard Strøm, David Grémillet, Maud Brault-Favrou, Arnaud Tarroux, Sébastien Descamps, Vegard Sandøy Bråthen, Benjamin Merkel, Jens Åström, et al.

Seabirds reveal mercury distribution across the North Atlantic

Céline Albert[1*], Børge Moe[2], Hallvard Strøm[3], David Grémillet[4,5], Maud Brault-Favrou[1], Arnaud Tarroux[6], Sébastien Descamps[3], Vegard Sandøy Bråthen[2], Benjamin Merkel[3, a], Jens Åström[2], Françoise Amélineau[4, b], Frédéric Angelier[7], Tycho Anker-Nilssen[2], Olivier Chastel[7], Signe Christensen-Dalsgaard[2], Jóhannis Danielsen[8], Kyle Elliott[9], Kjell Einar Erikstad[6], Alexey Ezhov[10], Per Fauchald[6], Geir W. Gabrielsen[3], Maria Gavrilo[11, 12], Sveinn Are Hanssen[6], Hálfdán H. Helgason[3, c], Malin Kjellstadli Johansen[3], Yann Kolbeinsson[13], Yuri Krasnov[10], Magdalene Langset[2], Jérémy Lemaire[1], Svein-Håkon Lorentsen[2], Bergur Olsen[8], Allison Patterson[9], Christine Plumejeaud-Perreau[1], Tone K. Reiertsen[6], Geir Helge Systad[14], Paul M. Thompson[15], Thorkell Lindberg Thórarinsson[13], Paco Bustamante[1, 16], Jérôme Fort[1*]

Corresponding authors *: Dr Céline Albert celine_albert567@hotmail.com and Dr Jérôme Fort jerome.fort@univ-lr.fr

I**nstitutions:**

[1] Littoral, Environnement et Sociétés (LIENSs), UMR 7266 CNRS-La Rochelle Université, 2 Rue Olympe de Gouges, 17000 La Rochelle, France

[2] Norwegian Institute for Nature Research (NINA), Høgskoleringen 9, 7034 Trondheim, Norway

[3] Norwegian Polar Institute (NPI), Fram Centre, Hjalmar Johansens Gate 14, 9296 Tromsø, Norway

[a] Akvaplan-niva, Fram Centre, Hjalmar Johansens gate 14, NO-9007 Tromsø, Norway

[4] Centre d'Ecologie Fonctionnelle et Evolutive (CEFE) UMR 5175, CNRS – Université de Montpellier – Université Paul-Valéry Montpellier – EPHE, 34293 Montpellier, France

[5] FitzPatrick Institute of African Ornithology, UCT, Rondebosch 7701, South Africa

[6] Norwegian Institute for Nature Research (NINA) Fram Centre, Hjalmar Johansens Gate 14, 9296 Tromsø, Norway

[7] Centre d'Etudes Biologiques de Chizé (CEBC), UMR 7372 CNRS La Rochelle Université, 405 Rte de Prissé la Charrière, 79360 Villiers-en-Bois France

[8] Faroe Marine Research Institute, Nóatún 1, FO-100 Tórshavn, Faroe Islands

[9] Department of Natural Resource Sciences, McGill University, Ste Anne-de-Bellevue, QC H9X 3V9, Canada

[10] Murmansk Marine Biological Institute, 17 Vladimirskaya street, 183010 Murmansk, Russia

[11] Association Maritime Heritage, RU – 199106, Icebreaker "Krassin", The Lieutenant Schmidt emb., 23 Line, Saint-Petersburg, Russia

[12] Arctic and Antarctic Research Institute, Saint-Petersburg, RU 199397

[13] Northeast Iceland Nature Research Centre, Hafnarstétt 3, 640 Húsavík, Iceland

[14] Norwegian Institute for Nature Research (NINA), Thormøhlensgate 55, N0-5006 Bergen, Norway

[15] University of Aberdeen, School of Biological Sciences, Lighthouse Field Station, Ross-shire, Cromarty IV11 8YJ, Scotland

[16] Institut Universitaire de France (IUF), 1 rue Descartes, 75005 Paris, France

Current affiliation:

[b] Ecosystèmes, biodiversité, évolution (ECOBIO), UMR 6553 CNRS - Université de Rennes 1, Rue de Thabor 35000 Rennes, France

[c] East Iceland Nature Research Centre, 700 Egilsstaðir, Iceland

Contributions

Conceptualisation: JF, CA

Sample and data contribution: AT, SD, VSB, MBF, BM, FA, FA, TAN, OC, SCD, JD, KE, EEK, AE, MG, GWG, SAH, YK, YK, ML, SHL, OB, AP, TKR, GHS, PMT, TLT, PB, JF

Data coordination and management: CA, JF, BM, VSB, HHH, MJ

Laboratory analyses: CA, MBF, JL, JF

Statistical methodology, CA, JF, SD, BM, JÅ, AT, VSB, BS

Writing the manuscript: CA, JF

Supervision: JF

Editing the manuscript: all authors.

Abstract

Mercury (Hg) is a heterogeneously distributed toxicant affecting wildlife and human health. Yet, the spatial distribution of Hg remains poorly documented, especially in food webs, even though this knowledge is essential to assess large-scale risk of toxicity for the biota and human populations. Here, we used seabirds to assess, at an unprecedented population and geographic magnitude and high resolution, the spatial distribution of Hg in North Atlantic marine food webs. To this end, we combined tracking data of 837 seabirds from seven different species and 27 breeding colonies located across the North Atlantic and Atlantic Arctic together with Hg analyses in feathers representing individual seabird contamination based on their winter distribution. Our results highlight an east-west gradient in Hg concentrations with hot spots around southern Greenland and the east coast of Canada and a cold spot in the Barents and Kara Seas. We hypothesize those gradients are influenced by eastern (Norwegian Atlantic Current and West Spitsbergen Current) and western (East Greenland Current) oceanic currents and melting of the Greenland Ice Sheet. By tracking spatial Hg contamination in marine ecosystems and through the identification of areas at risk of Hg toxicity, this study provides essential knowledge for international decisions about where the regulation of pollutants should be prioritized.

Significance statement

Mercury (Hg) causes deleterious effects on wildlife and human health. Even though we know Hg is heterogeneously distributed, its spatial distribution at very large-scale in the marine biota remains poorly documented. Seabirds are commonly used to study the health of marine environments. In this study, we used seabirds as bioindicators of Hg presence through the North-Atlantic Arctic. Our maps highlight a gradient in Hg concentrations, with

concentrations increasing from the Barents Sea to the East coast of Canada. This work is of tremendous importance for Arctic communities who rely on the marine environment but also for international initiatives such as the Minamata Convention that actively work for decreasing Hg emissions worldwide.

Introduction

Mercury (Hg), under its most toxic form (methyl-mercury, MeHg), is a toxicant that bioaccumulates and biomagnifies[1], affects wildlife and human health and is globally distributed in both marine and terrestrial environments[2]. The spatial distribution of Hg in marine systems is largely heterogeneous, due to a wide-range of abiotic transportation processes and contrasting local environmental conditions and biogeochemistry[3–5]. Recent investigations provided new insights on the oceanic and atmospheric distribution of Hg[6–9]. Coastal areas' Hg concentrations are mostly influenced by rivers[10], whereas offshore, they are mostly affected by oceanic and atmospheric depositions[11]. However, our knowledge about Hg spatial distribution in food webs remains limited (but see[12–14]), often with a coarse resolution or restricted to coastal regions[2,12,15–17]. Such knowledge and the subsequent identification of Hg hot and cold spots (i.e., areas with the highest and lowest concentrations, respectively) is nonetheless essential to assess large-scale exposure of species and support their management, and to protect communities, like the Arctic Indigenous peoples, who rely on top predators for subsistence. The mapping of the spatial distribution of Hg will also improve the understanding of Hg cycling and its transfer into food webs, as well as provide essential knowledge for international efforts aiming to reduce Hg in the environment. For instance, the Minamata Convention on Mercury aims to "protect human health and the environment from anthropogenic emissions and releases of mercury and mercury compounds"[18]. But to assess the effectiveness of the Minamata Convention and potential changes in Hg release, we first need to track spatial variation of Hg in biota and identify where the hot and cold spots are to

identify risks and manage major sources of Hg emissions. In this context, top predators like seabirds are powerful bio-monitors of spatial variation of Hg levels[19–21]. Seabirds have a wide distribution, occupying all marine regions of the globe[22]. They use a variety of marine habitats (e.g. coastal and oceanic, pelagic and benthic) and can be tracked in space and time using miniaturized electronic devices[23–27]. The geolocation technology allows us to relate Hg concentrations in specific individuals to their at-sea distribution and thus provide detailed information about environmental Hg for areas that are otherwise difficult to access[15,23]. In this study, we simultaneously tracked the spatial winter distribution of 837 seabirds belonging to seven species breeding at 27 colonies across the North Atlantic (i.e. Eastern Canada, Greenland, Iceland, Scotland, Faroe Islands, Norway, Western Russian Arctic) and their individual winter contamination with Hg measured in feathers. Our aim was to provide new insights into Hg spatial distribution and hot and cold spots within marine food webs at the North Atlantic scale. As coastal and offshore areas do not have the same sources of Hg, we used a multi-species approach which includes a wide range of life history traits (foraging ecology, trophic position) known to affect seabird Hg uptake, thus providing the most comprehensive spatial distribution of Hg.

Seabirds as indicators of mercury distribution in North Atlantic food-webs

Mercury concentrations varied along both longitudes and latitudes (**Table S1**, **Fig 1B; Fig S1B**), with a general positive east-west gradient across the North Atlantic. Results from our ocean-scale data extend previous investigations for the North Atlantic and sub-Arctic which suggested higher coastal Hg concentrations off eastern Canada compared to European coasts[19,20,28]. Beyond this general pattern, our approach provides the first in situ evidence that Hg distribution in biota was largely heterogeneous at fine-scale and across the entire oceanic North Atlantic (**Fig. 1B**). Previous work mapped MeHg in phytoplankton worldwide, but this

was a modelling work based on abiotic observations and transfer of MeHg at the base of the food chain only[29]. In the present study, highest concentrations occurred in Hg hot spots located along the eastern Canadian coasts as well as off the southern and southeastern coasts of Greenland. Mercury concentrations, in feathers representing contamination at these hot spots, were found to be up to three time as high as in the Barents and Kara Seas (minimum-maximum estimated values 1.55-4.05µg g^{-1} dry weight). Additionally, cold spots where Hg concentrations measured in feathers were the lowest were found in waters west of Iceland, around Jan Mayen, on the north Norwegian coast and in the White Sea.

Identifying the large-scale distribution of Hg in marine ecosystems is possible through large at-sea sampling campaigns. Such programs (e.g., GEOTRACES) exist and have proven their importance for the understanding of contaminant eco-dynamics[5,30,31]. Nonetheless, they are particularly costly and logistically difficult to implement and maintain over time. Therefore, complementary approaches such as the use of bioindicators that provide information about the contamination status of an environment are essential. To efficiently inform about Hg contamination in marine environment, the chosen bioindicator species are usually top predators (i.e., highest concentration of Hg due to biomagnification process), long-lived (i.e., highest concentration of Hg due to bioaccumulation process) and widely distributed (i.e., cover different and large environments)[22,26,27]. With this study, we demonstrate how the use of Hg measurements in seabird feathers combined with biologging (tracking data) can be used to identify Hg hot spots and cold spots at large spatial scale (see[15,16] for previous species- and population-specific investigations). Over the last two decades, the improvement of tracking technologies (e.g. smaller and lighter devices, battery autonomy) has allowed scientists to follow seabird movements and distribution outside the breeding period (e.g., the SEATRACK database, https://seapop.no/en/seatrack/ and associated publications[23,24,26], BirdLife Seabird Tracking Database

https://www.seabirdtracking.org and associated publication[27,32] http://www.seabirdtracking.org). The collection of feather samples from bioindicators, like seabirds that integrate Hg contamination over a period (e.g., seasonal or yearly contamination[28]), allows for concurrent measurements of Hg concentrations (see network ARCTOX https://arctox.cnrs.fr/en/home/[4,23]) at very large-scale and high resolutions that cannot easily be done by research vessels that can only make *ad hoc* measurements. With their global distribution, seabirds are thus excellent candidates for a global investigation of Hg distribution in marine ecosystems. In addition, these *in situ* approaches and their outputs are essential to complement and feed modelling approaches[29]. We nonetheless stress that almost all seabird species are feeding within the epipelagic zone (<200 m depth) and thus can only be used to quantify the spatial distribution of Hg in this water layer. Previous investigations showed the heterogeneous distribution of Hg along the water column and a dependence on its stratification[33,34]. Other bioindicators, such as marine mammals or predatory fishes, that can also be tracked to follow environmental conditions in space and time[33] could be considered as good bioindicators for deeper stratification layers. For instance, large-scale variations in Hg concentrations were shown in the Tropical Pacific using skipjack tuna (*Katsuwonus pelamis*)[12]. Similarly, seabirds have previously been used to highlight differences in Hg exposure between different regions at the species and population level, and thus suggested spatial differences in environmental contamination (e.g., [16,35] in the North Pacific, [15] in the North Atlantic). However, those studies were species specific and therefore covered only a limited compartment of the environment (e.g., specific habitat and diet). Multi-species analysis, in contrast, allows us to cover different ecologies, spanning multiple habitats and diets.

Spatial origin of mercury in marine environment and seabird conservation

The underlying drivers of the spatial variability seen in the present study are not well understood, but two hypotheses can be made. Firstly, the presence of Hg in oceanic currents could explain the east-west difference. In the North Atlantic, ascendant oceanic currents circulating along the Norwegian and Spitsbergen coasts transport 43 ± 9 Mg y-1 (i.e., gross flux) of Hg to the Arctic, where it accumulates with a residence time of 50 to 100 years[36]. Similarly, 54 ± 13 Mg y^{-1} of Hg is exported south by descendant oceanic currents from the Arctic to southern Greenland passing along the East coast of Greenland before flowing up its west coast[37]. This high export of Hg from the Arctic could explain the increased concentrations of Hg measured in the eastern and southern parts of Greenland. Secondly, the melting of the Greenland Ice Sheet could release Hg from geological sources, resulting in high concentrations of Hg along the south coasts of Greenland [3839]. Mercury is also deposited on ice sheets and snow through the Arctic because of atmospheric deposition[40] and then released into the marine environment during periods of melting[36,41]. These multiple sources of Hg in North Atlantic and Arctic marine systems strengthen the need to use multiple seabird species that rely on oceanic and/or coastal, pelagic and/or benthic environments to derive a more comprehensive understanding about Hg distribution in biota. Finally, because Hg contamination mostly originates from diet and consumed prey, bird species, which have different trophic ecology, were included as a random factor in the statistical and spatial analyses so that it would not bias Hg spatial distribution (See Methods). Doing so, seabirds were specifically used as bioindicators of Hg contamination. Characterizing hot spots of Hg in marine ecosystems is essential to highlight areas where the marine biota may be at risk of toxicity. By combining existing tracking data from multiple seabird species in the North Atlantic, major hot spots of biodiversity have been identified in the middle of the North Atlantic, and by the Great Bank and northwards into the Labrador Sea [27,42]. In our present study, model outputs show that these western areas had some of the highest predictions for Hg

contamination which implies a higher toxicity risk compared to the biota wintering in the eastern part of the North Atlantic. Acknowledging the existence of high risk of Hg contamination within these hot spots strengthens the need for protecting these areas. Based on these hot spots of biodiversity, the OSPAR commission has recently established a marine protected area in the middle of the North Atlantic[27]. However, because of the high transportability of Hg at a large spatial scale, it is international regulations like the Minamata Convention, that entered into force in 2017 and have been ratified by over 145 parties to date, that can act to strengthen the decrease of Hg emissions. The evaluation of the efficiency of associated mitigation measures requires a monitoring of Hg both in the environment and in food webs. By providing information at large spatial and temporal scales, and with a high resolution[15,16], our data thus fill an important knowledge gap and complement existing studies regarding Hg distribution in water masses [29,37], in biota[11] and international programs such as the Global Mercury Assessment led by UN Environment[2].

Societal and stakeholder implications

Arctic human communities mostly rely on traditional food resources, usually top predators, exposing them to high Hg concentrations. Consequently, the Arctic Indigenous Peoples possess some of the highest human concentrations of Hg worldwide[36,43]. Various deleterious effects have been found with for instance neurological deficits in children or cardiovascular disease in adults[44]. The Hg concentrations measured in the Greenlandic and Canadian Inuit populations are among the highest measured in the Arctic and are in accordance with our results[44]. Therefore, as our study gives new insight about the spatial distribution of Hg through the North Atlantic, we urge 1) the international community to take new actions to protect both the environment and human health from Hg toxicity as presented within the Minamata Convention, and 2) international programs to coordinate a global action

towards an improved knowledge of Hg monitoring in marine ecosystems. The assessment of the biota in the open sea is a complicated endeavour, as species migrate and are not easily accessible. However, this study and our technical approach of tracking and sampling feathers of seabirds have proved its efficiency to assess Hg contamination where seabirds are at sea. Our work demonstrates how wildlife can be used as cost-efficient bioindicators to gather important and new information about Hg distribution at a large scale. Such information is essential for the international community to take new and rapid action regarding the contamination by Hg of the environment and the subsequent risk for wildlife, human health and the environment.

Acknowledgements

This study is part of several research programs supported by the French Agency for National Research (MAMBA project ANR-16-TERC-0004, ILETOP, project ANR-16-CE34-0005, ARCTIC-STRESSORS project, ANR-20-CE34-0006), the French Arctic Initiative – CNRS, (PARCS project), the Mission pour l'Interdisciplinarité − CNRS (Changements en Sibérie project), the French Polar Institute (IPEV – Pgr 388 ADACLIM, Pgr 330 ORNITO-ENDOCRINO) and the European Commission (Marie Curie CIG, Project 631203). This study is part of the long-term Studies in Ecology and Evolution (SEE-Life) program of the CNRS. The IUF (Institut Universitaire de France) is also acknowledged for its support to P.B. as a Senior Member. C.A. was supported by a PhD fellowship from the French Ministry of Higher Education and Research. Thanks to the CPER (Contrat de Projet Etat-Région) and the FEDER (Fonds Européen de Développement Régional) for funding the AMA (Advanced Mercury Analyser) of LIENSs laboratory. We thank the plateforme analytique of the Institute of Littoral, Environment and Societies (LIENSs). The deployment and retrieval of GLS-loggers and sampling of feathers were conducted as part of the SEATRACK project (www.seapop.no/en/ seatrack/) in northern Europe (Norwegian and UK colonies), made possible through close cooperation with the SEAPOP program (www.seapop.no, Norwegian Research Council grant #192141) and the ARCTOX network (https://arctox.cnrs.fr/en/home/).

METHODS

Species, study sites and sample collection

From June-July 2014 to June-July 2017 chick rearing Atlantic puffins (*Fratercula arctica*, n = 42), black-legged kittiwakes (*Rissa tridactyla*, n = 119), Brünnich's guillemots (thick-billed murres; *Uria lomvia*, n = 239), common guillemots (common murres; *Uria aalge*, n = 131), little auks (dovekies; *Alle alle*, n = 64), northern fulmars (*Fulmarus glacialis*, n = 124) and incubating common eiders (*Somateria mollissima*, n = 118), were outfitted with light-level geolocators (GLS – Global Location Sensor) at 27 breeding colonies, for one to four years during the breeding season. These colonies were distributed across the northern part of the North Atlantic (**Table S1**), encompassing Eastern Canada, Greenland, Iceland, Scotland, Faroe Islands, Norway and Western Russian Arctic (**Fig. 1A**). The outfitted seabirds were of undetermined sex for all species but common eiders, for which only females were studied. GLSs were retrieved in each subsequent breeding season (one to four retrievals per individual in the period 2015 to 2018) (**Table S2**). At each GLS retrieval, three feathers per individual (either from head, back or belly) were collected for subsequent Hg analyses[15,23,28,45]. Collected feathers were selected to represent Hg contamination during the non-breeding period (i.e. from approx. October to February, see "*Hg analyses*" below), a period comparable to that actually spent at the wintering grounds (i.e. from approx. November to January, see "*Spatial analyses*" below) and successfully used in previous research [15,23]. Non-breeding periods include migration. We assumed that Hg accumulated at stopovers and acquired along migration routes (a few days within the October-February period[24]) could be neglected in comparison to Hg accumulated over the about five months spent at wintering grounds. Feather collection and GLS deployments/retrieval were mostly done as part of the ARCTOX network (https://arctox.cnrs.fr/en/home/) and SEATRACK (https://seapop.no/en/seatrack/) project which aim to track Hg contamination across Arctic

marine food webs and model the non-breeding distribution of seabirds breeding throughout the North Atlantic, respectively. Mercury concentrations in coastal areas are mostly influenced by river[10], whereas offshore areas are mostly affected by oceanic and atmospheric depositions[11]. Therefore, we used species that use either coastal (i.e., common eiders) or offshore environment (i.e., Atlantic puffins, black-legged kittiwakes, Brünnich's guillemots, common guillemots, little auks, northern fulmars). Additionally, we used species that feed at the surface (black-legged kittiwakes, northern fulmars) or on benthic preys (common eiders), or feed on epipelagic prey down to 50–150 m depth, depending on the birds' body size (in increasing order: little auks, Atlantic puffins, Brünnich's guillemots and common guillemots).

Spatial analyses

GLS light-level data were converted into a positional dataset by identifying the timing of twilights, using a threshold method[45], from which two daily latitudes and longitudes were estimated from apparent day- and night-lengths and from time of midnight and noon, respectively (see[46] for details). The accuracy of locations estimated from light-level data is usually considered as low, and it is recommended to use such data to study movements > 200 km[46–48]. Low accuracy is mainly due to errors in latitude and less so in longitudes, when light conditions are affected by factors such as weather, habitat, topography, behavior and artificial light. Further, constant daylight and polar night prevent estimation of location. When using a light threshold corresponding to sun elevation angles around -3° to -4°, this occurs above 63°N and 70°N at summer and winter solstice, respectively[48]. In addition, latitudes are increasingly unreliable closer to spring or autumn equinox, when the day length is similar at all latitudes on the planet. We therefore discarded latitude during a three-week period on each side of the apparent equinox (8 September – 20 October and 20 February – 3 April) for all species.

To mitigate these multiple issues, we first applied several filters to improve timing of twilights, to remove the most erroneous locations, as described in[49]. Then, we applied an informed random movement algorithm (IRMA[50]) to fill the data gaps (including during the equinoxes) by modelling a maximum of two random locations per day. This method follows an approach originally proposed by[51], and takes into account complementary information on light levels, land masks to replace the missing locations with the most plausible estimates, thereby reducing the sampling bias in our dataset to the minimum possible[50]. More specifically, in winter the model uses information about land and sea-ice masks (constraining random positions to areas with <80% sea-ice concentration), whether the logger recorded a continuous night (constraining the seabird to north of the limit of the polar night area), and species-specific movement rates (constrain each new location to remain within a certain distance to adjacent locations). IRMA is parametrized for offshore, pelagic species only and is not suitable for common eiders that are benthic species relying on coastal environments. Hence, IRMA could not be used for this particular species, for which the positional gaps were not corrected.

To link Hg contamination to areas with the most extensive feeding through the winter season, we excluded the post and pre-breeding periods. Thus, we considered the winter period to be the same within species as the timing of seabirds' non-breeding period is small[24,52–54] and should not affect Hg spatial distribution. Therefore, we defined the winter period as the period November to January for Atlantic puffins (see[24]), black-legged kittiwakes[55], Brünnich's and common guillemots[53,56,57], common eiders[58] and little auks[54]. As northern fulmars have been returning to their colonies as early as January in the literature[59], which was also observed in our dataset (**Fig. S1**), the non-breeding period was defined from November to December for this species (SEATRACK, *Unpublished*). Although individual seabirds show a rather restricted distribution during winter at the scale of the North Atlantic, they can show

small-scale changes in their spatial distribution[24]. To take this small-scale winter spatial distribution into account, a medoid winter location (i.e., the location with the shortest and - nearest neighbor distance - to all the other locations of a given track) was calculated per week, for each individual and for their entire winter period (mean values of positions per species and sampling sites are presented in **Table S1**).

Mercury analyses

Feathers were used as indicators of individual Hg contamination during winter, when seabirds are at sea[28]. Briefly, during their molt, seabirds excrete ~70–90% of accumulated Hg into their feathers[60–62]. Hence, Hg in feathers inform about the Hg accumulated by an individual between two molting sequences. Alcids and Larids undergo a total molt after the breeding season (i.e. right before, during or right after the post-breeding migration, September – October) resulting in the winter plumage, and a partial molt (i.e., cheek, neck, throat for Alcids, back and head for Larids) at the end of the non-breeding period (i.e. right before or during the pre-nuptial migration, March - April) resulting in the nuptial plumage[63,64]. Female common eiders undergo a partial molt (i.e. body contour feathers) after the breeding season, and a complete molt at the end of the non-breeding period[65,66]. Hence, head, back and belly feathers provide information about Hg contamination specifically during the non-breeding period in alcids, black-legged kittiwakes and common eiders, respectively. Northern fulmars undergo one total molt per year after the breeding season (body feathers molted between September and March[67]). Recent studies indicated that Hg concentrations in body feathers of northern fulmars reflect inter-individual variations in Hg contamination during the winter period[67]. Consequently, and in order to investigate Hg contamination during the non-breeding period, we collected in the following breeding season head feathers from Atlantic puffins, Brünnich's guillemots, common guillemots and little auks, back feathers from black-legged

kittiwakes, and belly feathers from common eiders and northern fulmars. Feathers were stored in plastic bags at ambient temperature until Hg analyses.

Prior to Hg analyses, feathers were cleaned to remove external contamination. To do so, they were plunged into a 2:1 chloroform:methanol solution for three minutes in an ultrasonic bath, rinsed twice in a methanol solution and dried at 45°C for 48 hours. Mercury analyses were performed on a ~ 0.20-1.00 mg subsample of a pool of three homogenized feathers (i.e. to avoid heterogeneity between feathers), using an Advanced Mercury Analyzer spectrophotometer (Altec AMA 254 – detection limit of 0.05 ng). The analysis of each sample was repeated (two to three times) until the relative standard deviation for two subsamples was <10%. Mean concentration for these two subsamples was then used for statistical analyses. Prior to Hg analyses, blanks were run and, to ensure the accuracy of measurements, certified reference materials were used every fifteen samples (lobster hepatopancreas TORT-3; NRC, Canada; reference values were of 0.29 ± 0.02 µg g^{-1} dry weight (dw) *SD* (i.e., Standard Deviation), mean measured ± *SD* = 0.30 ± 0.002 µg g^{-1} dw, recovery = 102.0 ± 1.5 %; and lobster hepatopancreas TORT-2; 0.27 ± 0.06 µg g^{-1} dw *SD*, mean measured = 0.26 ± 0.01 µg g^{-1} dw *SD*, recovery = 97.3 ± 1.0%). Mercury concentrations are expressed in µg g^{-1} dry weight (dw). Total Hg concentrations are used as proxies of MeHg as more than 80% of the Hg excreted into feathers is under its organic and toxic MeHg form[68,69].

Statistical analyses

Mercury spatial distribution in the North Atlantic was predicted by regression-kriging (RK) (using package "*gstat*"[70]). Within the different regression-kriging methods, we used the ordinary-kriging (hereafter OK)[71]. This technique is based on a spatial interpolation on a surface that uses the closest cell to calculate its prediction in each cell and allows to use regression models. More specifically, as we want to use seabirds as bioindicators (i.e.,

homogenise the different ecologies), this method allowed us to use mixed models to add species as random effects. The regression-kriging technique consists of two steps. The first step uses linear regression to model the spatial trends in the dataset and the second step interpolate the residuals from the linear regression using kriging. The final spatial predictions on the surface are the sum of the predictions from the two steps.

***Step 1*:** applying a regression (linear mixed model - LMM) and predict Hg concentrations at the medoid winter locations. Our full model was: Hg ~1 + fixed effects (longitude + latitude) + random effects (species : sampling sites). All seabird species were included in the model and "species" was included as a random effect. This allow us to take into account their different ecologies in the model (e.g., habitat, prey) and therefore use seabirds as bioindicators only. Indeed, during the non-breeding period seabirds rely on different habitats where Hg concentrations are under different influences[10,40] and prey. Food is the main pathway for Hg accumulation in seabirds[72]. Therefore, and due to biomagnification processes[73], contrasting diet, trophic status and habitats (both between populations and species) might affect measured Hg concentrations and need to be taken into account in the model. However, the use of seabirds with different ecologies as bioindicators could have some limitations. Our models captured the dataset heterogeneity as shown for instance by the ICC (see below). A common method in ecology to take into account different ecologies consists of using carbon and nitrogen stable isotopes. However, this method could not be applied here as stable isotopes do not cover the same period as Hg contamination in feathers[74]. Indeed, while Hg concentrations in feathers represent an inter-molt period, the stable isotope values only represent the period of the feather growth. Additionally, as our study is based on a multi-colony analysis, colonies ("sampling sites") were included as a random effect to take into account the different breeding distributions and the different non-breeding strategies (e.g., length of migration - **Fig. S2**). As several species can breed at a

sampling site, we have nested the variable "species" into the variable "sampling site". The Intraclass Correlation Coefficient (ICC) indicates that 64 – 69% of the variances in Hg concentrations comes from the variables "species" and "sampling site". For each winter, individuals had one Hg concentrations for one to 14 winter location (see "*Spatial analyses"*) and 212 individuals (15 Atlantic puffins, 8 black-legged kittiwakes, 72 Brünnich's guillemots, 25 common eiders, 39 common guillemots, 7 little auks and 46 northern fulmars) have been sampled for 2 to 4 years (see **Table S1**). To take into account the individual variability and non-independence of this variable, we used a bootstrap approach (i.e., random extraction – see details below in ***step 2***), which allowed us to exclude "individual' from the linear mixed model. This random extraction of the data was necessary as individuals were attributed to several (weekly) non-breeding medoid points (see "*Spatial analyses"*) making this variable non-independent.

Step 2: We summed the predictions from the LMM and OK. More specifically, we used the residuals of the LMMs to run the interpolation with the OK on a 1° x 1°grid covering the entire North Atlantic (**Figs. 1B-S3**)[75]. The use of the residuals of the LMM to run the kriging analyses is the most common method of regression kriging, and allows us to include the spatial variability of our dataset that is not captured by the LMM[71]. The use of regression kriging requires that one or more covariates (here longitude and latitude of the medoid winter locations) are significantly correlated with the dependent variable (i.e., Hg concentrations) to ensure the strength between the response and predictive variables, which was the case (correlation coefficient (2.5 - 97.5 quantiles): -0.47 - -0.43, p-value (2.5 - 97.5 quantiles): 4.9e-48 - 1.3e-39; correlation coefficient (2.5 - 97.5 quantiles): -0.38 - -0.35, p-value (2.5 - 97.5 quantiles): 4.9e-31 - 3.2e-21; respectively).

In order to take the lack of independence in our data into account (i.e., repeated individual positions), we used a bootstrap approach (i.e., random extraction) (**Fig. 2**). To do

so, we randomly extracted one medoid position per individual to create a subset of independent data. We repeated this procedure 1000 times to create a total of 1000 subsets. On each subset, we ran the two steps of the regression kriging method and calculated the predicted values from both the LMM and the OK. After that, we were able to sum both predictions from the LMM and OK to get improved predictions[76].

The final output is a map of the mean predictions from each subset (**Figures 1B-S3**). A map of the variance calculated for all the predictions is also provided in appendix (**Fig S3**). It presents the variance between our 1000 subsamples. To determine the minimally sufficient number of subsets to account for the heterogeneity of our dataset, and this validate our approach using 1000 subsets, we calculated the variance between each final map each time we added an iteration until we reached a stable variance (**Figures 2 & S4**).

Mercury concentrations (the LMM response variable) were log transformed to meet the parametric assumptions of normality and homoscedasticity of the residual distributions. Statistical analyses were performed with R version 3.4.3 and RStudio version 1.3.1093[77]. Means are reported with standard deviation (mean ± *SD*) unless reported otherwise.

Captions

Figure 1. A) Winter distribution (weekly medoid locations from November to January for Atlantic puffins, black-legged kittiwakes, Brünnich's guillemots, common eiders, common guillemots and little auks, and from November to December for Northern fulmars) colored by species (colored points) and breeding colonies (black points). **B)** Predictions of the estimated Hg concentrations (in log) for 1000 iterations (see *Methods*) with highest values in dark blue and lowest predictions in yellow.

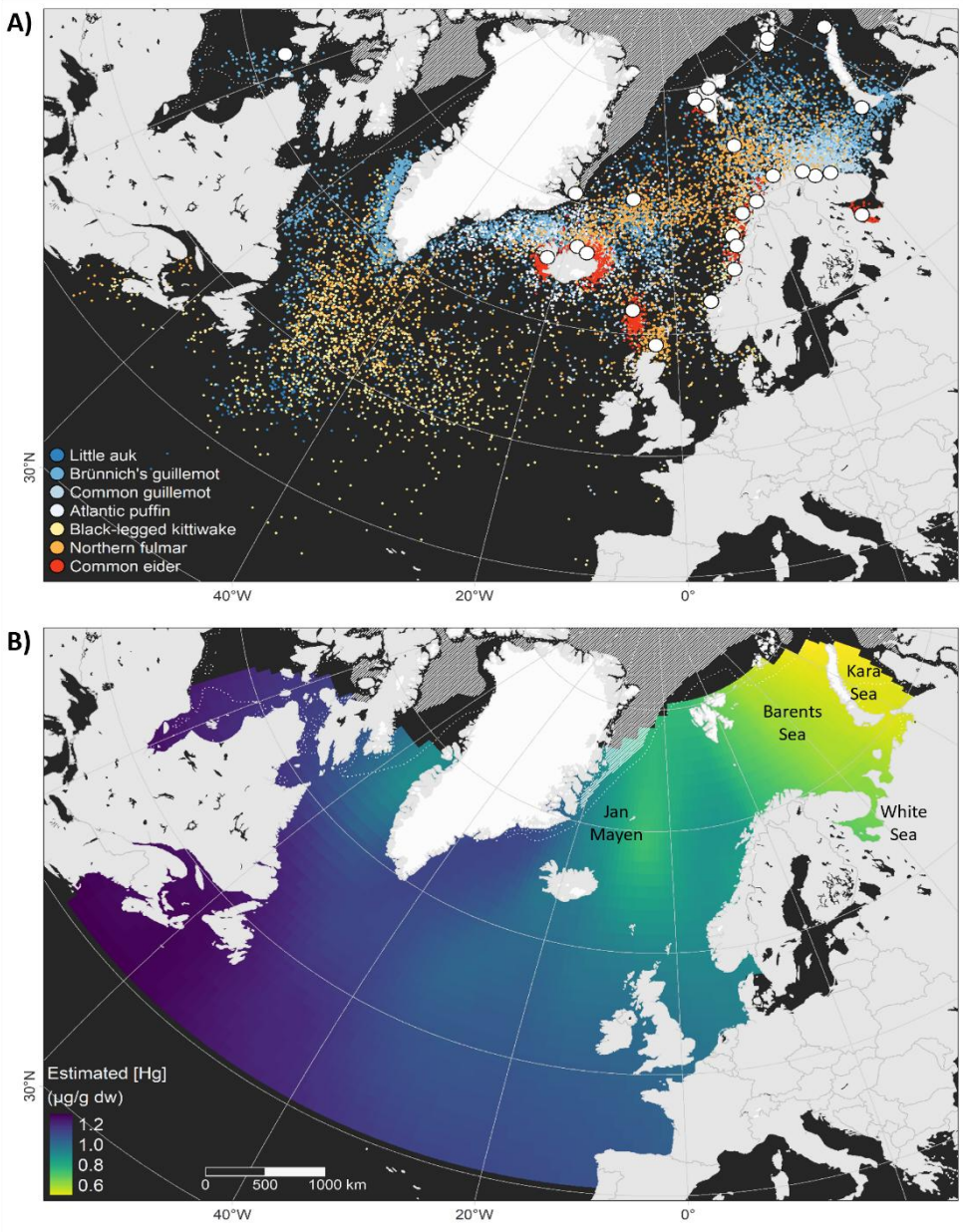

Figure 2. Schematic description of the statistical analyses with **1)** data preparation, **2)** regression kriging with step 1 (regression) and step 2 (ordinary kriging) and **3)** mapping of model predictions (estimated Hg concentrations).

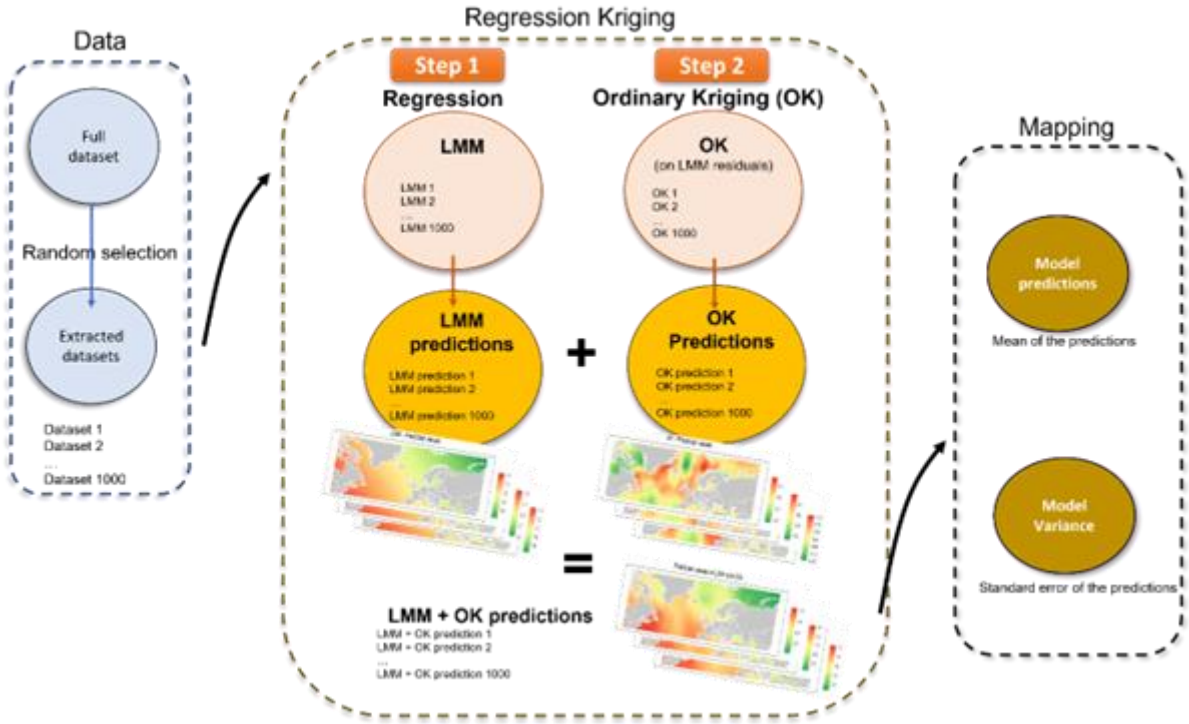

Bibliography (Main text 1-42, Methods 43-74)

1. Morel, F. M. M., Kraepiel, A. M. L. & Amyot, M. The chemical cycle and bioaccumulation of mercury. *Annual Review of Ecology and Systematics* **29**, 543–566 (1998).
2. UN Environment Programme. *Global Mercury Assessment 2018*. (2019).
3. Jiskra, M. *et al.* Mercury stable isotopes constrain atmospheric sources to the ocean. *Nature* **597**, 678–682 (2021).
4. Renedo, M. *et al.* Contrasting spatial and seasonal trends of methylmercury exposure pathways of Arctic seabirds: Combination of large-scale tracking and stable isotopic approaches. *Environ. Sci. Technol.* **54**, 13619–13629 (2020).
5. Heimbürger, L.-E. *et al.* Shallow methylmercury production in the marginal sea ice zone of the central Arctic Ocean. *Sci. Rep.* **5**, (2015).
6. Pomerleau, C. *et al.* Pan-Arctic concentrations of mercury and stable isotope ratios of carbon (δ13C) and nitrogen (δ15N) in marine zooplankton. *Sci. Total Environ.* **551–552**, 92–100 (2016).
7. Bowman, K. L., Hammerschmidt, C. R., Lamborg, C. H., Swarr, G. J. & Agather, A. M. Distribution of mercury species across a zonal section of the eastern tropical South Pacific Ocean (U.S. GEOTRACES GP16). *Mar. Chem.* **186**, 156–166 (2016).
8. Wang, K. *et al.* Subsurface seawater methylmercury maximum explains biotic mercury concentrations in the Canadian Arctic. *Sci. Rep.* **8**, (2018).
9. Dastoor, A. *et al.* Arctic atmospheric mercury: Sources and changes. *Science of The Total Environment* **839**, 156213 (2022).
10. Liu, M. *et al.* Substantial accumulation of mercury in the deepest parts of the ocean and implications for the environmental mercury cycle. *Proc. Natl. Acad. Sci. U.S.A.* **118**, e2102629118 (2021).
11. AMAP. *AMAP Assessment 2018: Biological Effects of Contaminants on Arctic Wildlife and Fish.* vii+84pp (2018).
12. Médieu, A. *et al.* Evidence that Pacific tuna mercury levels are driven by marine methylmercury production and anthropogenic inputs. *Proc. Natl. Acad. Sci. U.S.A.* **119**, e2113032119 (2022).

13. Tseng, C.-M. *et al.* Bluefin tuna reveal global patterns of mercury pollution and bioavailability in the world's oceans. *Proc. Natl. Acad. Sci. U.S.A.* **118**, e2111205118 (2021).
14. Carravieri, A. *et al.* Trace elements and persistent organic pollutants in chicks of 13 seabird species from Antarctica to the subtropics. *Environ. Int.* **134**, 105225 (2020).
15. Fort, J., Robertson, G. J., Grémillet, D., Traisnel, G. & Bustamante, P. Spatial ecotoxicology: Migratory arctic seabirds are exposed to mercury contamination while overwintering in the Northwest Atlantic. *Environ. Sci. Technol.* **48**, 11560–11567 (2014).
16. Fleishman, A. B. *et al.* Wintering in the Western Subarctic Pacific increases mercury contamination of red-legged kittiwakes. *Environ. Sci. Technol.* (2019) doi:10.1021/acs.est.9b03421.
17. Azad, A. M. *et al.* Effects of geography and species variation on selenium and mercury molar ratios in Northeast Atlantic marine fish communities. *Sci. Total Environ.* **652**, 1482–1496 (2019).
18. United Nations Environment Programme. Minamata convention on mercury: text and annexes. (2013).
19. Provencher, J. F., Mallory, M. L., Braune, B. M., Forbes, M. R. & Gilchrist, H. G. Mercury and marine birds in Arctic Canada: Effects, current trends, and why we should be paying closer attention. *Environ. Rev.* **22**, 244–255 (2014).
20. AMAP. *AMAP Assessment 2002: Heavy Metals in the Arctic*. (AMAP, Oslo, 2005).
21. Albert, C. *et al.* Seasonal variation of mercury contamination in Arctic seabirds: A pan-Arctic assessment. *Sci. Total Environ.* **750**, 142201 (2021).
22. Harrison, P. *Seabirds: An Identification Guide*. (Croom Helm, London, 1983).
23. Albert, C. *et al.* Inter-annual variation in winter distribution affects individual seabird contamination with mercury. *Mar. Ecol. Prog. Ser.* **676**, 243–254 (2021).
24. Amélineau, F. *et al.* Six pelagic seabird species of the North Atlantic engage in a fly-and-forage strategy during their migratory movements. *Mar. Ecol. Prog. Ser.* **676**, 127–144 (2021).
25. Clairbaux, M. *et al.* North Atlantic winter cyclones starve seabirds. *Curr. Biol.* **31**, 3964-3971.e3 (2021).
26. Fauchald, P. *et al.* Year-round distribution of Northeast Atlantic seabird populations: applications for population management and marine spatial planning. *Mar. Ecol. Prog. Ser.* **676**, 255–276 (2021).

27. Davies, T. E. *et al.* Multispecies tracking reveals a major seabird hotspot in the North Atlantic. *Conserv. Lett.* **14**, (2021).
28. Albert, C., Renedo, M., Bustamante, P. & Fort, J. Using blood and feathers to investigate large-scale Hg contamination in Arctic seabirds: A review. *Environ. Res.* **177**, 108588 (2019).
29. Zhang, Y., Soerensen, A. L., Schartup, A. T. & Sunderland, E. M. A global model for methylmercury formation and uptake at the base of marine food webs. *Glob. Biogeochem. Cycles* **34**, (2020).
30. Cossa, D. *et al.* Mercury distribution and transport in the North Atlantic Ocean along the GEOTRACES-GA01 transect. *Biogeosci. Discuss.* 1–36 (2017) doi:10.5194/bg-2017-467.
31. Cossa, D. *et al.* Sources, cycling and transfer of mercury in the Labrador Sea (G eotraces -G eovide cruise). *Mar. Chem.* **198**, 64–69 (2018).
32. Clark, B. L. Global assessment of marine plastic exposure risk for oceanic birds. *Nature Communications* (2023).
33. Roquet, F. *et al.* A Southern Indian Ocean database of hydrographic profiles obtained with instrumented elephant seals. *Sci. Data* **1**, 140028 (2014).
34. Carravieri, A., Cherel, Y., Jaeger, A., Churlaud, C. & Bustamante, P. Penguins as bioindicators of mercury contamination in the southern Indian Ocean: geographical and temporal trends. *Environ. Pollut.* **213**, 195–205 (2016).
35. Shoji, A. *et al.* Geolocators link marine mercury with levels in wild seabirds throughout their annual cycle: Consequences for trans-ecosystem biotransport. *Environ. Pollut.* **284**, 117035 (2021).
36. AMAP. *AMAP Assessment 2021: Mercury in the Arctic. Arctic Monitoring and Assessment Programme (AMAP), Tromsø, Norway.* https://www.amap.no/documents/doc/amap-assessment-2021-mercury-in-the-arctic-uncorrected-proofing-draft/3581 (2021).
37. Petrova, M. V. *et al.* Mercury species export from the Arctic to the Atlantic Ocean. *Mar. Chem.* **225**, 103855 (2020).
38. Hawkings, J. R. *et al.* Large subglacial source of mercury from the southwestern margin of the Greenland Ice Sheet. *Nat. Geosci.* **14**, 496–502 (2021).

39. Jørgensen, C. J. *et al.* Large mercury release from the Greenland Ice Sheet invalidated. *Sci. Adv.* **10**, eadi7760 (2024).
40. AMAP. *AMAP, 2011. Snow, Water, Ice and Permafrost in the Arctic (SWIPA): Climate Change and the Cryosphere.* (2011).
41. Sonke, J. E. *et al.* Eurasian river spring flood observations support net Arctic Ocean mercury export to the atmosphere and Atlantic Ocean. *Proc. Natl. Acad. Sci. U. S. A.* 201811957 (2018) doi:10.1073/pnas.1811957115.
42. Yurkowski, D. J. *et al.* Abundance and species diversity hotspots of tracked marine predators across the North American Arctic. *Divers. Distrib.* **25**, 328–345 (2019).
43. Basu, N. *et al.* A State-of-the-Science Review of Mercury Biomarkers in Human Populations Worldwide between 2000 and 2018. *Environ. Health Perspect.* **126**, 106001 (2018).
44. Basu, N. *et al.* The impact of mercury contamination on human health in the Arctic: A state of the science review. *Sci. Total Environ.* **831**, 154793 (2022).
45. Lavoie, R. A. *et al.* Contamination of mercury during the wintering period influences concentrations at breeding sites in two migratory piscivorous birds. *Environmental Science & Technology* **48**, 13694–13702 (2014).
46. Lisovski, S. *et al.* Light-level geolocator analyses: A user's guide. *J. Anim. Ecol.* **89**, 221–236 (2020).
47. Bråthen, V. S. *et al. An Automated Procedure (v2.0) to Obtain Positions from Light-Level Geolocators in Large-Scale Tracking of Seabirds. A Method Description for the SEATRACK Project. NINA Report 1893. Norwegian Institute for Nature Research, Trondheim.* https:// brage. nina. no/ nina-xmlui/handle/11250/2735757 (2021).
48. Bråthen, V. S. *et al. Processing of Light-Level Geolocator Data into a Basic Positional Dataset for the SEATRACK-Project. Unpublished Manuscript*. (2020).
49. Lisovski, S. *et al.* Geolocation by light: accuracy and precision affected by environmental factors: *Accuracy of geolocation by light*. *Methods Ecol. Evol.* **3**, 603–612 (2012).

50. Fauchald, P. *et al. Arctic-Breeding Seabirds' Hotspots in Space and Time - A Methodological Framework for Year-Round Modelling of Environmental Niche and Abundance Using Light-Logger Data*. http://hdl.handle.net/11250/2595504.
51. Technitis, G., Othman, W., Safi, K. & Weibel, R. From A to B, randomly: a point-to-point random trajectory generator for animal movement. *Int. J. Geogr. Inf. Sci.* **29**, 912–934 (2015).
52. Fort, J. *et al.* Multicolony tracking reveals potential threats to little auks wintering in the North Atlantic from marine pollution and shrinking sea ice cover. *Divers. Distrib.* **19**, 1322–1332 (2013).
53. Frederiksen, M. *et al.* Migration and wintering of a declining seabird, the thick-billed murre Uria lomvia, on an ocean basin scale: Conservation implications. *Biol. Conserv.* **200**, 26–35 (2016).
54. Fort, J., Beaugrand, G., Grémillet, D. & Phillips, R. A. Biologging, remotely-sensed oceanography and the continuous plankton recorder reveal the environmental determinants of a seabird wintering hotspot. *PLoS ONE* **7**, e41194 (2012).
55. Frederiksen, M. *et al.* Multicolony tracking reveals the winter distribution of a pelagic seabird on an ocean basin scale: Winter distribution of Atlantic kittiwakes. *Divers. Distrib.* **18**, 530–542 (2012).
56. Fort, J. *et al.* Energetic consequences of contrasting winter migratory strategies in a sympatric Arctic seabird duet. *J. Avian Biol.* **44**, 255–262 (2013).
57. Merkel, B. *et al.* Earlier colony arrival but no trend in hatching timing in two congeneric seabirds (Uria spp.) 2 across the North Atlantic. *Biol. Lett.* (2019).
58. Hanssen, S. A. *et al.* Migration strategies of common eiders from Svalbard: Implications for bilateral conservation management. *Polar Biol.* **39**, 2179–2188 (2016).
59. Macdonald, M. A. The winter attendance of fulmars at land in NE Scotland. *Ornis Scandinavica (Scandinavian Journal of Ornithology)* **11**, 23–29 (1980).
60. Honda, K., Nasu, T. & Tatsukawa, R. Seasonal changes in mercury accumulation in the black-eared kite, Milvus migrans Lineatus. *Environ. Pollut.* **42**, 325–334 (1986).
61. Braune, B. M. Comparison of total mercury levels in relation to diet and molt for nine species of marine birds. *Arch. Environ. Contam. Toxicol.* **16**, 217–224 (1987).

62. Agusa, T. *et al.* Body distribution of trace elements in Black-tailed gulls from Rishiri Island, Japan: age-dependent accumulation and transfer to feathers and eggs. *Environ. Toxicol. Chem.* **24**, 2107 (2005).
63. Cramp, S. & Simmons, K. E. L. *Handbook of the Birds of Europe, the Middle East and North Africa. The Birds of the Western Palearctic. Vil III. Waders to Gulls*. (Oxford University Press, Oxford, 1983).
64. Gaston, A. J. & Jones, I. L. *The Auks*. (Oxford University Press, 1998).
65. Baldassarre, G. Ducks, geese and swans of North America. *J. Wildl. Manag.* **79**, 1034–1035 (2015).
66. Goudie, R. I., Robertson, G. J. & Reed, A. Common Eider (Somateria mollissima), version 1.0. *In Birds of the World (S.M. Billerman, Editor)* (2020) doi:https://doi.org/10.2173/bow.comeid.01.
67. Quinn, L. R., Meharg, A. A., van Franeker, J. A., Graham, I. M. & Thompson, P. M. Validating the use of intrinsic markers in body feathers to identify inter-individual differences in non-breeding areas of northern fulmars. *Mar. Biol.* **163**, (2016).
68. Bond, A. L. & Diamond, A. W. Mercury concentrations in seabird tissues from Machias Seal Island, New Brunswick, Canada. *Sci. Total Environ.* **407**, 4340–4347 (2009).
69. Renedo, M. *et al.* Assessment of mercury speciation in feathers using species-specific isotope dilution analysis. *Talanta* **174**, 100–110 (2017).
70. Pebesma, E. J. Multivariable geostatistics in S: the gstat package. *Comput. Geosci.* **30**, 683–691 (2004).
71. Odeh, I. O. A., McBratney, A. B. & Chittleborough, D. J. Further results on prediction of soil properties from terrain attributes: heterotopic cokriging and regression-kriging. *Geoderma* **67**, 215–226 (1995).
72. Carravieri, A. *et al.* Mercury exposure and short-term consequences on physiology and reproduction in Antarctic petrels. *Environ. Pollut.* **237**, 824–831 (2018).
73. Kim, E. Y. *et al.* Metal accumulation in tissues of seabirds from Chaun, northeast Siberia, Russia. *Environ. Pollut.* **92**, 247–252 (1996).
74. Bond, A. L. Relationships between stable isotopes and metal contaminants in feathers are spurious and biologically uninformative. *Environmental Pollution* **158**, 1182–1184 (2010).
75. Hengl, T., Heuvelink, G. B. M. & Rossiter, D. G. About regression-kriging: From equations to case studies. *Comput. Geosci.* **33**, 1301–1315 (2007).

76. Shi, T., Dirienzo, N., Requia, W. J., Hatzopoulou, M. & Adams, M. D. Neighbourhood scale nitrogen dioxide land use regression modelling with regression kriging in an urban transportation corridor. *Atmos. Environ.* **223**, 117218 (2020).
77. R Core Team. R: A language and environment for statistical computing. R Foundation for Statistical Computing (2017).

Supplementary information - Captions

Figure S1. Summarize for each species of: **A)** Winter distribution (weekly medoid locations from November to January for Atlantic puffins, black-legged kittiwakes, Brünnich's guillemots, common eiders, common guillemots and little auks, and from November to December for Northern fulmars); breeding colonies are identified by white black points. **B)** Predictions of the estimated Hg concentrations (in log) for 1000 iterations (see *Methods*) with highest values in dark blue and lowest predictions in yellow. **C)** Mapping of the variance (standard deviation) for each species (n = 1000 iterations) with the highest variance in dark brown and the lowest in light orange.

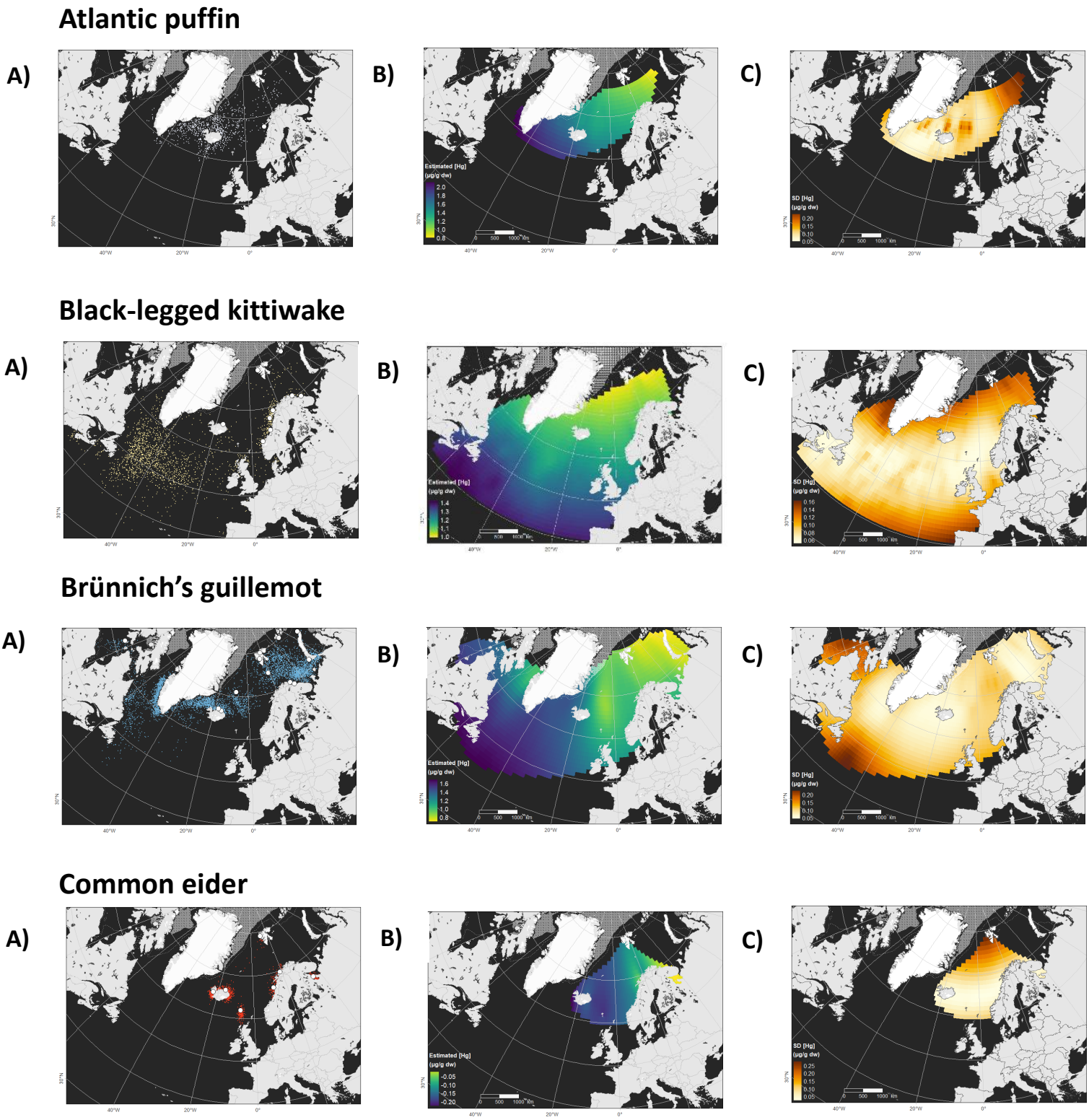

Common guillemot

A)

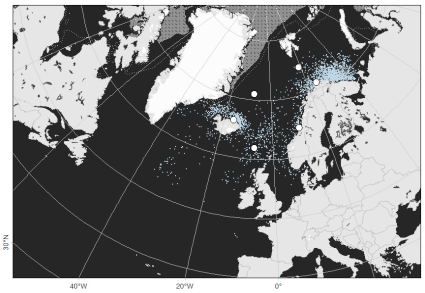

B)

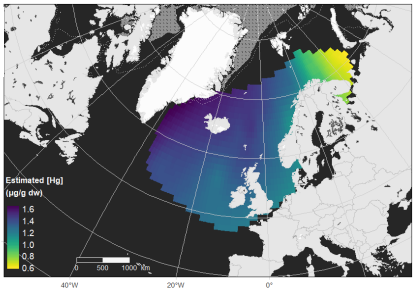

C)

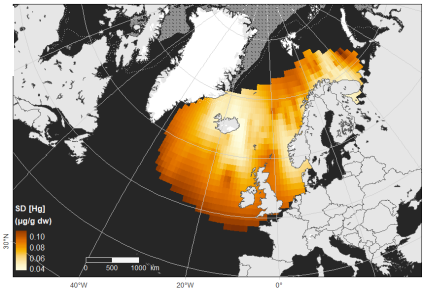

Little auk

A)

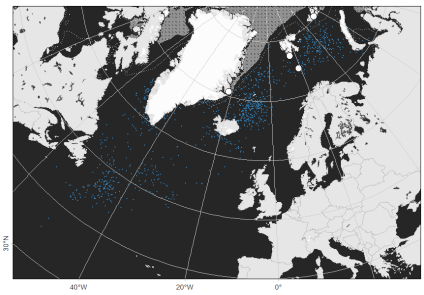

B)

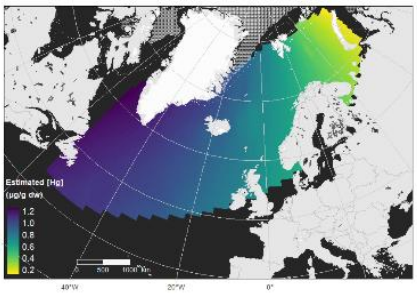

C)

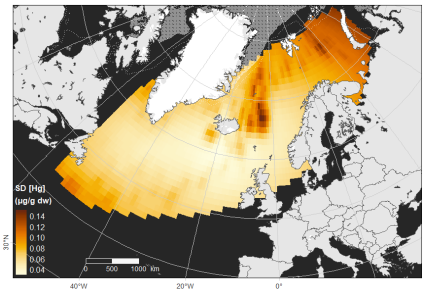

Northern fulmar

A)

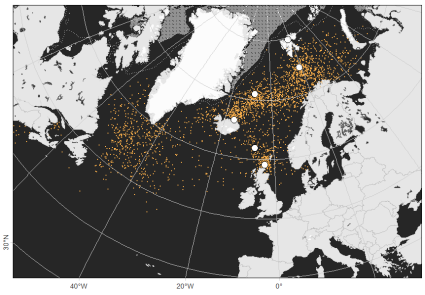

B)

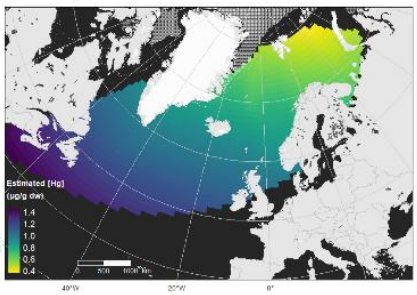

C)

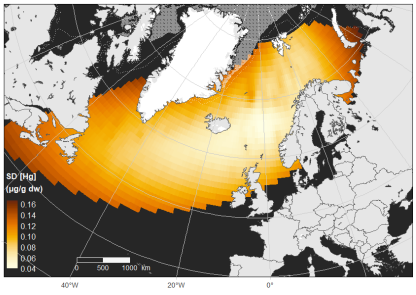

Figure S2. Plot of mean weekly distances away from the breeding colony to illustrate when each species can be expected to attend their respective wintering grounds. Blue solid vertical lines illustrate the months of November to January, where we assume most individuals attend their wintering grounds, except for the Northern fulmar, where we only include November and December (marked with a blue dotted vertical line), as many return to their breeding colony in January.

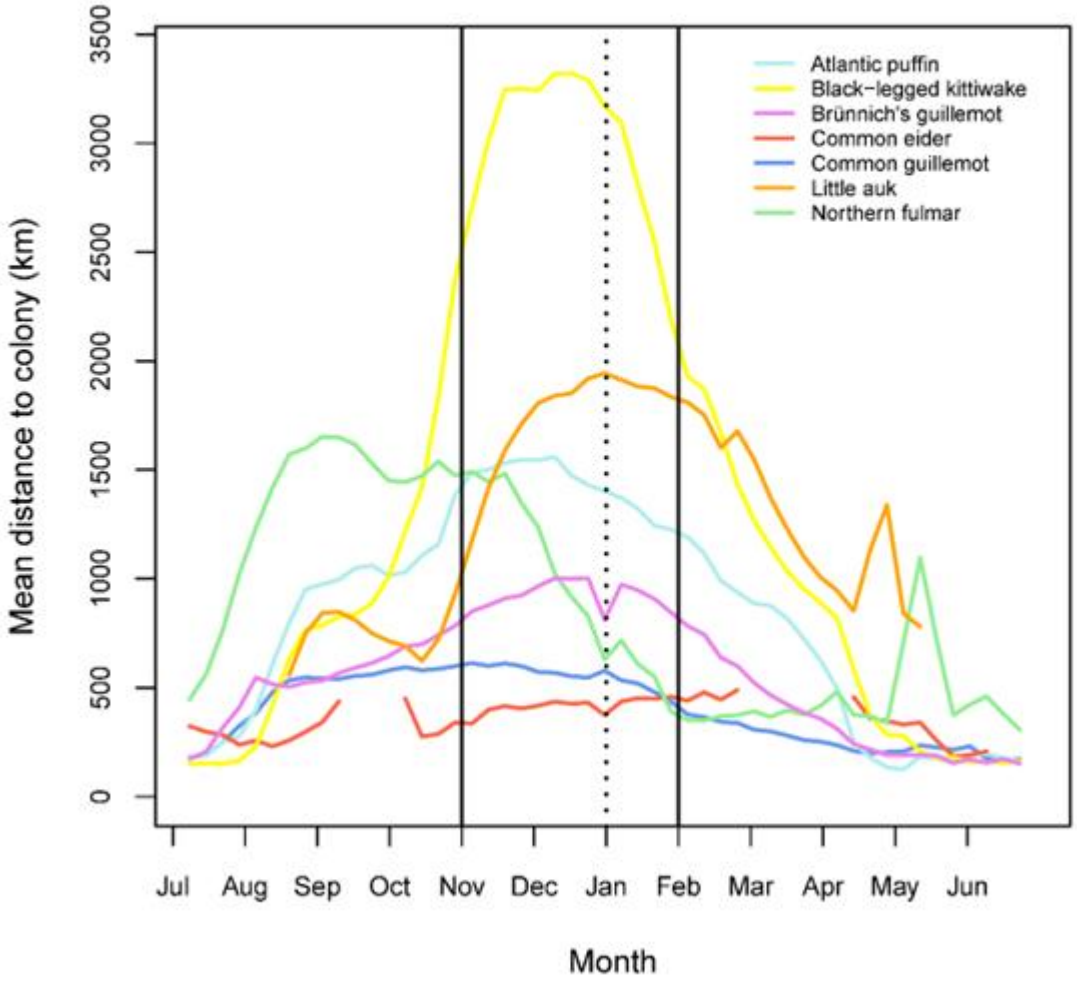

Figure S3. Mapping of the variance (standard deviation) for all the map of predictions (**Fig. 1B**) (n = 1000 iterations) with the highest variance in dark brown and the lowest in light orange

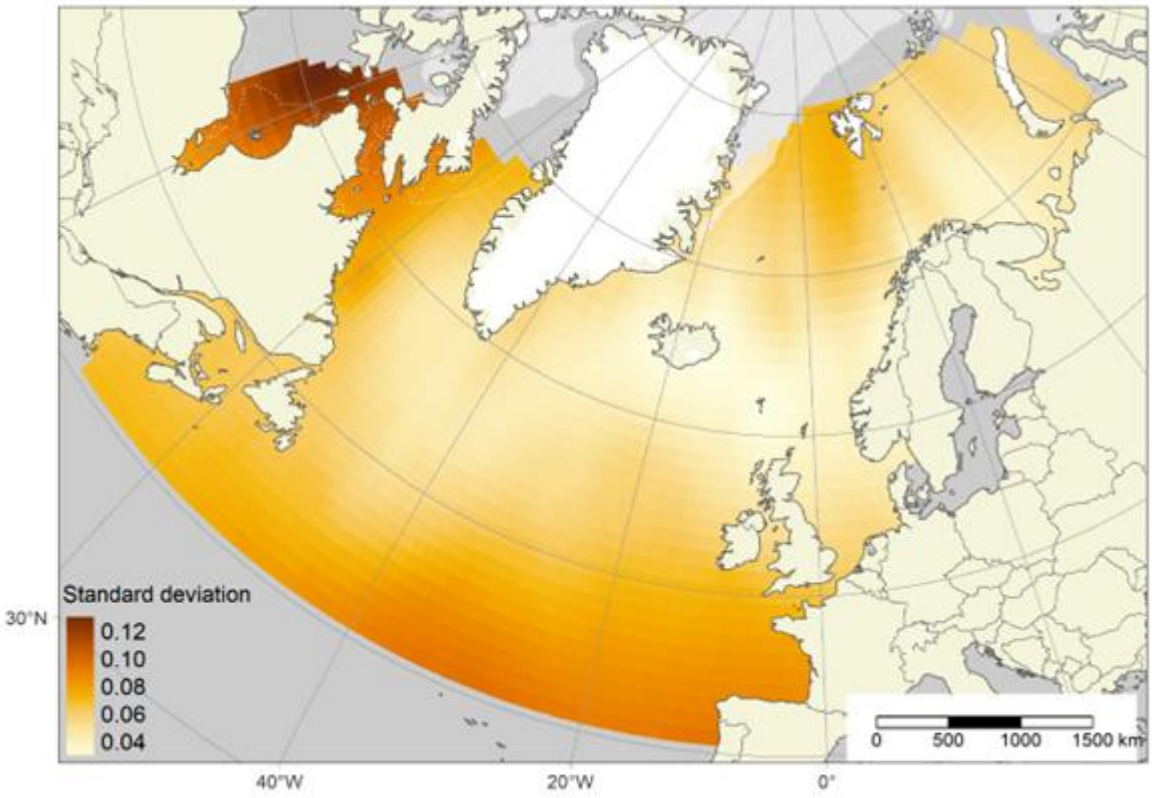

Figure S4. Mean of the variance (standard deviation) between each map regarding the number of iteration (n = 1000 iterations).

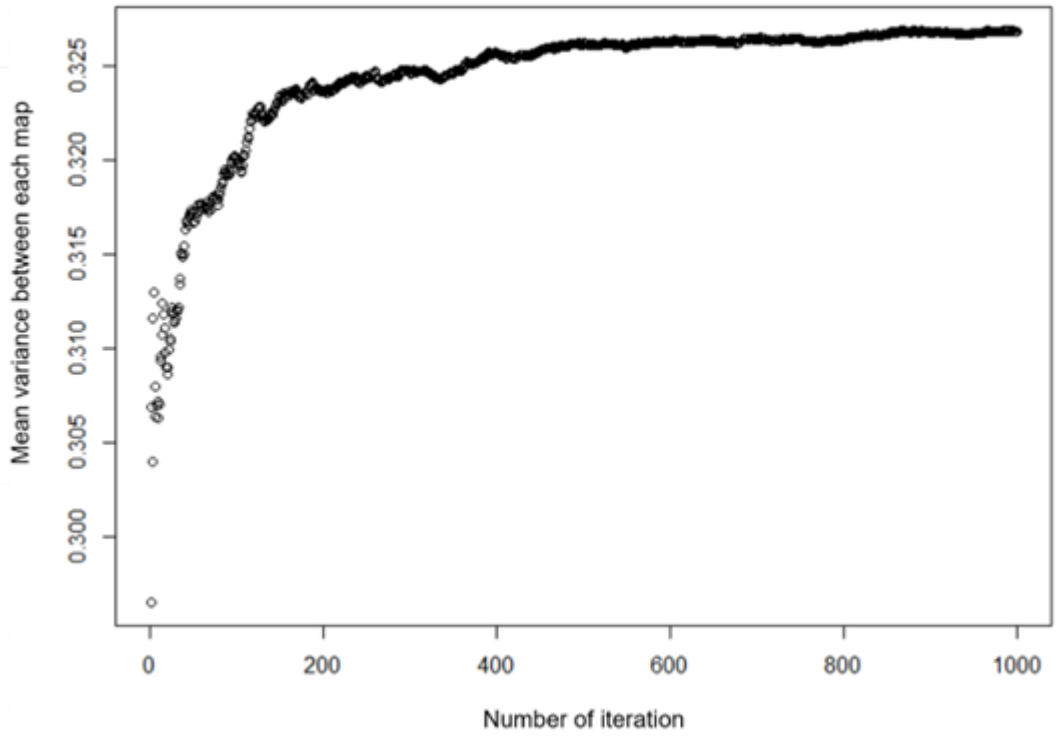

Table S1. Hg concentrations (in µg g^{-1} dw) measured in feathers (head feathers on Atlantic puffins, Brünnich's guillemots, common guillemots and little auks, back feathers on black-legged kittiwakes, and belly feathers on common eiders and northern fulmars), winter median longitude and latitude (mean ± SD), per species and sampling sites *(2015-2018 combined)*. Number of positions (see Methods) and individuals are also mentioned

Sampling colonies	Colonies coordinates	Species	Positions (n)	Hg measurements (n)	Individuals (n)	Winter [Hg]	Winter medoid Latitude	Winter medoid longitude
Alkefjellet	*79.58°N, 18.51°E*	Brünnich's guillemot	402	29	23	1.68 ± 0.45	76.04 ± 1.72	27.27 ± 10.53
		Northern fulmar	82	6	5	1.34 ± 0.97	73.57 ± 2.52	37.65 ± 12.24
Anda	*69.07°N, 15.17°E*	Black-legged kittiwake	294	21	19	3.37 ± 1.41	57.50 ± 7.10	-24.92 ± 24.70
Bjørnøya	*74.50°N, 18.96°E*	Brünnich's guillemot	559	40	25	2.95 ± 1.72	69.30 ± 3.04	-3.89 ± 17.70
		Common guillemot	789	58	32	2.09 ± 0.68	70.83 ± 1.34	34.17 ± 6.61
		Little auk	457	34	28	2.60 ± 1.07	67.59 ± 5.18	-14.03 ± 20.44
		Northern fulmar	543	39	22	1.49 ± 0.88	73.20 ± 1.83	22.18 ± 11.59
Breidafjordur	*65.08°N, 22.74 °W*	Common eider	252	18	10	0.96 ± 0.43	64.60 ± 0.57	-22.59 ± 0.82
Cape Flora	*79.95°N, 50.09°E*	Black-legged kittiwake	110	8	8	6.17 ± 2.04	53.27 ± 8.66	-35.26 ± 22.61
		Brünnich's guillemot	56	4	4	1.65 ± 0.35	75.86 ± 1.35	38.82 ± 6.41
Cape krutik	*69.15°N, 35.95°E*	Black-legged kittiwake	110	8	8	2.30 ± 0.85	56.34 ± 8.79	-30.27 ± 32.30
Kara gate	*62.47°N, 83.10°W*	Brünnich's guillemot	502	36	36	1.82 ± 0.50	70.53 ± 1.01	50.03 ± 6.21
Coats Island	*59.14°N, 3.12°W*	Brünnich's guillemot	315	23	23	4.39 ± 3.57	57.42 ± 4.43	-62.83 ± 11.98
Eynhallow	*61.98°N, 6.65°W*	Northern fulmar	342	25	20	3.72 ± 1.52	59.83 ± 4.34	-7.95 ± 15.86
Faroes		Common eider	285	21	17	0.65 ± 0.25	61.31 ± 0.81	-6.42 ± 0.65
		Common guillemot	97	7	7	5.13 ± 2.22	60.69 ± 4.53	-8.09 ± 8.47
	69.58°N, 32.94°E	Northern fulmar	165	12	12	3.46 ± 1.27	60.30 ± 5.08	-15.28 ± 18.60
Cape Gorodetskiy	*66.54°N, 18.00°W*	Brünnich's guillemot	97	7	7	2.12 ± 0.37	70.93 ± 1.65	28.95 ± 18.78
Grimsey	*71.11°N, 24.73°E*	Brünnich's guillemot	138	10	5	5.75 ± 0.83	61.95 ± 4.24	-40.50 ± 13.11
Hjelmsøya	*80.23°N, 53.02°E*	Common guillemot	382	28	21	3.02 ± 1.14	71.10 ± 1.02	30.20 ± 6.79
Hooker Island	*70.39°N, 31.16°E*	Little auk	221	17	16	1.53 ± 0.45	75.02 ± 2.83	30.61 ± 21.24
Hornøya		Black-legged kittiwake	138	10	10	2.40 ± 1.29	55.22 ± 5.98	-35.72 ± 22.18
	78.25°N, 15.51°E	Brünnich's guillemot	897	65	38	2.62 ± 1.17	70.35 ± 3.95	26.95 ± 27.01
Isfjorden		Brünnich's guillemot	224	17	14	6.25 ± 1.39	63.79 ± 4.69	-37.58 ± 16.04

	71.03°N, 8.29°W	Little auk	1	1	1	4.03	71.51	-8.89
Jan Mayen		Brünnich's guillemot	843	61	33	5.87 ± 1.81	64.10 ± 3.50	-39.46 ± 13.65
		Common guillemot	472	34	27	3.72 ± 1.48	67.66 ± 4.23	3.00 ± 25.51
	70.72°N, 21.55°W	Northern fulmar	648	47	33	2.73 ± 1.22	67.07 ± 6.56	-10.38 ± 19.04
Kap Höegh	*71.42°N, 51.95°E*	Little auk	254	19	19	3.00 ± 0.62	50.04 ± 5.07	-40.92 ± 8.47
Kongsfjorden	*79.00°N, 11.67°E*	Black-legged kittiwake	242	18	15	6.65 ± 2.43	51.76 ± 7.39	-34.93 ± 17.73
		Common eider	504	37	28	1.03 ± 0.33	66.34 ± 2.62	-12.10 ± 9.34
Langanes	*66.18°N, 15.99°W*	Black-legged kittiwake	203	15	15	5.57 ± 3.09	52.41 ± 5.42	-36.69 ± 10.23
		Brünnich's guillemot	417	30	25	4.88 ± 1.16	64.86 ± 3.05	-29.54 ± 13.57
		Common eider	184	16	16	1.07 ± 0.44	64.65 ± 0.61	-22.53 ± 0.83
		Common guillemot	517	37	27	3.72 ± 0.85	64.97 ± 2.32	-14.24 ± 8.04
		Northern fulmar	722	52	32	2.84 ± 1.22	62.49 ± 7.49	-26.26 ± 22.65
Oranskyi islands	*77.07°N, 67.64°E*	Brünnich's guillemot	84	6	6	1.73 ± 0.20	73.95 ± 2.11	45.80 ± 10.86
Røst	*67.45°N, 11.91°E*	Atlantic puffin	764	57	42	5.01 ± 1.94	66.47 ± 3.59	-17.35 ± 15.67
		Black-legged kittiwake	263	19	16	3.10 ± 1.15	57.51 ± 7.84	-22.98 ± 27.36
Runde Alesund	*62.44°N, 5.87°E*	Black-legged kittiwake	151	11	11	4.86 ± 1.28	53.55 ± 5.85	-30.25 ± 21.55
Selvaer	*66.59°N, 12.23°E*	Common eider	112	8	8	0.91 ± 0.24	66.10 ± 1.23	12.07 ± 1.32
Sklinna	*64.74°N, 10.77°E*	Black-legged kittiwake	234	17	17	2.14 ± 0.70	55.44 ± 6.56	-24.53 ± 22.18
		Common guillemot	234	17	17	3.21 ± 0.81	65.90 ± 5.09	16.44 ± 11.59
Solovetsky archipelago	*65.05°N, 35.79°E*	Common eider	223	16	15	1.23 ± 0.28	64.98 ± 0.89	36.27 ± 1.14
Tromsø	*69.64°N, 18.85°E*	Common eider	389	28	24	0.78 ± 0.76	69.16 ± 0.56	19.28 ± 1.14

Table S2. Number of geolocators deployed, retrieved and downloaded per species and year. The number of individuals used in the present study, per year and in total is also shown. "<2015" includes geolocators deployed before 2015

Species		<2015	2015	2016	2017	2018
Black-legged kittiwake	n GLS deployed	-	205	217	-	-
	n GLS retrieved	-	-	133	164	-
	n GLS successfully downloaded	-	-	128	154	-
	Studied individuals	-	0	71	40	0
Brünnich's guillemot	n GLS deployed	307	278	303	48	-
	n GLS retrieved	-	108	178	172	39
	n GLS successfully downloaded	-	101	157	156	35
	Studied individuals	-	82	135	116	23
Common eider	n GLS deployed	173	167	207	-	-
	n GLS retrieved	-	59	91	125	-
	n GLS successfully downloaded	-	49	72	100	-
	Studied individuals	-	24	62	81	0
Common guillemot	n GLS deployed	188	172	184	-	-
	n GLS retrieved	-	107	99	116	-
	n GLS successfully downloaded	-	95	74	95	-
	Studied individuals	-	60	48	80	0
Atlantic puffin	n GLS deployed	-	-	66	35	-
	n GLS retrieved	-	-	-	41	39
	n GLS successfully downloaded	-	-	-	34	30
	Studied individuals	-	0	0	31	28
Little auk	n GLS deployed	119	84	89	-	-
	n GLS retrieved	-	33	22	38	-
	n GLS successfully downloaded	-	30	19	37	-
	Studied individuals	-	8	15	29	0
Northern fulmar	n GLS deployed	176	143	169	-	-
	n GLS retrieved	-	69	88	89	-
	n GLS successfully downloaded	-	65	75	87	-
	Studied individuals	-	41	68	81	0